d^0/f^n-Mediated Ring-Opening Ziegler Polymerization (ROZP) and Copolymerization with Mono- and Disubstituted Methylenecyclopropanes. Diverse Mechanisms and a New Chain-Capping Termination Process

Tryg R. Jensen, James J. O'Donnell III, and Tobin J. Marks*

Department of Chemistry, Northwestern University, Evanston, Illinois 60208-3113

Received May 30, 2003

The mono- and disubstituted methylenecyclopropane derivatives 2-phenyl-1-methylenecyclopropane (**A**) and 7-methylenebicyclo[4.1.0]heptane (**B**) have been successfully implemented in ring-opening Ziegler polymerization. Homogeneous ethylene + 2-phenyl-1-methylenecyclopropane (**A**) random copolymerizations are mediated efficiently by the single-site catalysts $Cp^*_2ZrMe^+B(C_6F_5)_4^-$, $[Cp^*_2LuH]_2$, $[Cp^*_2SmH]_2$, and $[Cp^*_2YH]_2$ ($Cp^* = C_5Me_5$) to produce a copolymer (**C**) with **A** enchained in a ring-opened fashion. Single-site coordinative polymerization of 7-methylenebicyclo[4.1.0]heptane (**B**) proceeds via either ring-opened or ring-unopened pathways. In the presence of $Cp^*_2ZrMe^+$ $MeB(C_6F_5)_3^-$ at 0 °C, **B** undergoes polymerization to afford the insoluble, *ring-unopened* homopolymer **D**, which was characterized by CPMAS NMR, DSC, elemental analysis, FTIR, TGA, and XRD. The melting point of polymer **D** lies above its decomposition temperature (>300 °C). Random copolymerizations of **B** and ethylene mediated by $Cp^*_2ZrMe^+MeB(C_6F_5)_3^-$ at room temperature result in polymer **E**, a polyethylene capped by a ring-opened **B** fragment. The formation of **B**-capped polymer **E** is a consequence of a new chain transfer mechanism, as evidenced by a linear relationship between M_n and $[\mathbf{B}]^{-1}$. The rate constant for insertion of ethylene is ∼25× greater than the rate constant for insertion of monomer **B** into the metal−alkyl bond. Random copolymers (**F**) of ring-opened **B** and ethylene are produced when the catalysts $Me_2Si(Me_4C_5)(^tBuN)ZrMe_2$, $Me_2Si(Me_4C_5)(^tBuN)TiMe_2$ (activated by either $(C_6H_5)_3C^+$ $B(C_6F_5)_4^-$ or $B(C_6F_5)_3$), and $[Cp^*_2LuH]_2$ are employed.

Introduction

Electrophilic d^0/f^n metallocene centers are highly efficient catalysts for a variety of carbon−carbon bond-forming and bond-breaking transformations.[1,2] An unusual example is the d^0/f^n metallocene-mediated ring-opening Ziegler polymerization (ROZP) of strained methylenecycloalkanes in which sequential double-bond insertions and β-alkyl shift ring openings afford polyolefins with reactive *exo*-methylene functionalities (eq 1).[3] ROZP is a distinctive example of a polymerization in which a monomer undergoes enchainment followed by isomerization, with the process continuously repeating itself. Of particular interest is that the resulting polymer has well-regulated and reactive functional groups arrayed along the polyolefin backbone. This process thus provides an alternative approach to the formidable challenge of introducing functional groups on polyolefins besides "masked"[4] and borane-function-

---

[1] For recent reviews of metallocenium d^0 polymerization catalysis, see the following and references therein: (a) Gibson, V. C.; Spitzmesser, S. K. *Chem. Rev.* **2003**, *103*, 283. (b) Pedeutour, J.-N.; Radhakrishnan, K.; Cramail, H.; Deffieux, A. *Macromol. Rapid Commun.* **2001**, *22*, 1095. (c) Gladysz, J. A., Ed. *Chem. Rev.* **2000**, *100* (special issue on "Frontiers in Metal-Catalyzed Polymerization"). (d) *Advances in Polymerization Catalysis. Catalysts and Processes*; Topics in Catalysis 7; Marks, T. J., Stevens, J. C., Eds.; Baltzer: Red Bank, NJ, 1999. (e) Scheirs, J.; Kaminsky, W. *Metallocene-Based Polyolefins: Preparation, Properties, and Technology*; Wiley: New York, 1999; Vols. 1 and 2. (f) Kaminsky, W. *Metalorganic Catalysts for Synthesis and Polymerization: Recent Results by Ziegler-Natta and Metallocene Investigations*; Springer-Verlag: Berlin, 1999. (g) Britovsek, G. J. P.; Gibson, V. C.; Wass, D. F. *Angew. Chem., Int. Ed.* **1999**, *38*, 428. (h) McKnight, A. L.; Waymouth, R. M. *Chem. Rev.* **1998**, *98*, 2587 (constrained-geometry polymerization catalysts). (i) Jordan, R. F. *J. Mol. Catal.* **1998**, *128* (special issue on "Metallocene and Single Site Olefin Catalysis"). (j) Kaminsky, W.; Arndt, M. *Adv. Polym. Sci.* **1997**, *127*, 144. (k) Bochmann, M. *J. Chem. Soc., Dalton Trans.* **1996**, 255. (l) Brintzinger, H. H.; Fischer, D.; Mülhaupt, R.; Rieger, B.; Waymouth, R. M. *Angew. Chem., Int. Ed. Engl.* **1995**, *34*, 1143. (m) Soga, K., Terano, M., Eds. *Catalyst Design for Tailor-Made Polyolefins*; Elsevier: Tokyo, 1994.

[2] For recent reviews of f^n catalysis, see the following and references therein: (a) *Topics in Organometallic Chemistry*; Kobayashi, S., Ed.; Springer: Berlin, Germany, 1999; Vol. 2. (b) Molander, G. A. *Chemtracts: Org. Chem.* **1998**, *18*, 237. (c) Edelmann, F. T. *Top. Curr. Chem.* **1996**, *179*, 247. (d) Edelmann, F. T. In *Comprehensive Organometallic Chemistry*; Wilkinson, G., Stone, F. G. A., Abel, E. W., Eds.; Pergamon Press: Oxford, U.K., 1995; Vol. 4, Chapter 2. (e) Schumann, H.; Meese-Marktscheffel, J. A.; Esser, L. *Chem. Rev.* **1995**, *95*, 865. (f) Fu, P.-F.; Brard, L.; Li, Y.; Marks, T. J. *J. Am. Chem. Soc.* **1995**, *117*, 7157. (g) Schaverien, C. J. *Adv. Organomet. Chem.* **1994**, *36*, 283. (h) Shapiro, P. J.; Cotter, W. D.; Schaefer, W. P.; Labinger, J. A.; Bercaw, J. E. *J. Am. Chem. Soc.* **1994**, *116*, 4623. (i) Molander, G. A.; Hoberg, J. O. *J. Org. Chem.* **1992**, *57*, 3266. (j) Heeres, H. J.; Renkema, J.; Booji, M.; Meetsma, A.; Teuben, J. H. *Organometallics* **1988**, *7*, 2495. (k) Watson, P. L.; Parshall, G. W. *Acc. Chem. Res.* **1985**, *18*, 51. (l) Jeske, G.; Lauke, H.; Mauermann, H.; Schumann, H.; Marks, T. J. *J. Am. Chem. Soc.* **1985**, *107*, 8111.

[3] (a) Jia, L.; Yang, X. M.; Seyam, A. M.; Albert, I. D. L.; Fu, P. F.; Yang, S. T.; Marks, T. J. *J. Am. Chem. Soc.* **1996**, *118*, 7900. (b) Jia, L.; Yang, X. M.; Yang, S. T.; Marks, T. J. *J. Am. Chem. Soc.* **1996**, *118*, 1547. (c) Yang, X. M.; Seyam, A. M.; Fu, P. F.; Marks, T. J. *Macromolecules* **1994**, *27*, 4625. (d) Yang, X. M.; Jia, L.; Marks, T. J. *J. Am. Chem. Soc.* **1993**, *115*, 3392.

10.1021/om030407n CCC: $27.50

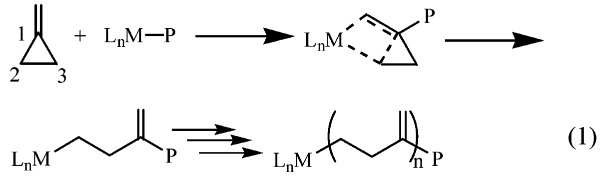

(1)

alized comonomer methodologies.[5] After examining a variety of electrophilic metal complexes, we succeeded in identifying catalysts capable of very selectively mediating the ring-opening Ziegler polymerization of methylenecyclopropane and methylenecyclobutane (eqs 2 and 3). Furthermore, methylenecyclopropane yields very diverse and interesting polymerization chemistry in the presence of other d^0/f^n metallocene centers. One catalyst yields a polyspirane at low temperatures (<−30 °C; eq 4) by first forming a ring-opened macromolecule and then effecting a cascade of ring-closing reactions via a “zipping-up” process. In contrast, larger ionic radius lanthanocene catalysts mediate the regioselective dimerization/cyclization of methylenecyclopropane to afford 1,2-dimethylene-3-methylcyclopentane (eq 5). Of potentially greater technological interest would be the ability to effect random copolymerizations of methylenecyclopropane or methylenecyclobutane with ethylene. It was shown that efficient random copolymer formation is mediated by a number of catalysts (Cp″ = 1,2-Me$_2$C$_5$H$_3$ and CGC = Me$_2$Si(Me$_4$C$_5$)(^{t}BuN)) competent for both methylenecyclopropane and methylenecyclobutane ring opening (eqs 6 and 7).

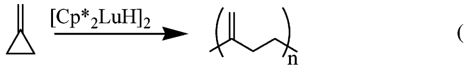

(2)

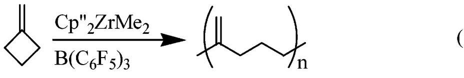

(3)

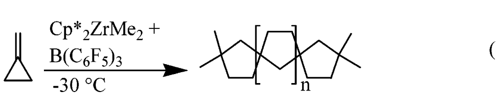

(4)

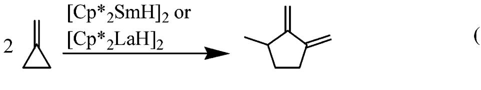

(5)

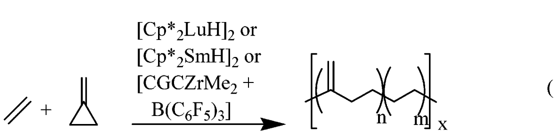

(6)

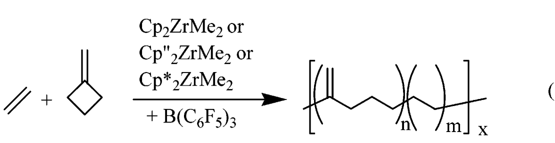

(7)

In contrast to the aforementioned results, recent reports on the homopolymerization of 2-phenyl-1-methylenecyclopropane (**A**) mediated by a variety of late-transition-metal catalysts suggest very different pathways.[6] Studies of the ring-opening polymerization of **A** mediated by Pd catalysts reveal, curiously, that the propagation mechanism (eq 8) follows an entirely different course than the ROZP of methylenecyclopropane mediated by d^0/f^n metallocene catalysts (eq 1).[6c] Furthermore, the Ni-catalyzed polymerization of **A** can be effected in either a completely ring-unopened fashion or to yield a mixture of ring-opened/ring-unopened **A** (ring-opened **A** comprising 45−63%).[6a,b] No copolymerization studies were reported for these systems.

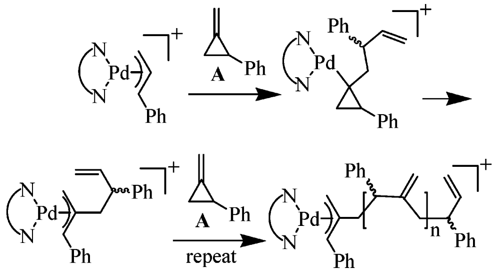

(8)

To further explore the scope and generality of ROZP, we have investigated the response of a variety of substituted methylenecyclopropanes to electrophilic d^0/f^n metallocene centers. In particular, we were interested in learning how substitution at the methylenecyclopropane skeletal positions 2 and 3 might influence the polymerization pathway. We report here our observations on the single-site polymerization and ethylene copolymerization characteristics of 2-phenyl-1-methylenecyclopropane (**A**) and 7-methylenebicyclo[4.1.0]heptane (**B**).[7] It will be seen here that while d^0/f^n metallocene catalysts are curiously ineffective in homopolymerizations of **A**, a variety of catalysts are competent to effect random copolymerization of **A** with ethylene to produce the new polymer **C**. Of particular note is that the ring-opening of the asymmetric methylenecyclopropyl ring with the proper choice of catalyst is completely selective for only one of two possible ring-opening pathways (while other catalysts produce a mixture). In contrast to these findings with **C**, polymerization of **B** can be effected in a ring-unopening mode to produce homopolymer **D**. However, we also show that copolymerizations of **B** with ethylene result in **B** ring-

A

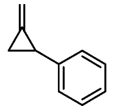

B

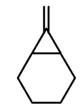

C

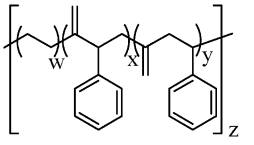

D

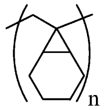

---

(4) (a) Kresti, M. R.; Coates, G. W.; Waymouth, R. M. *J. Am. Chem. Soc.* **1992**, *114*, 1025. (b) Imuta, J.-I.; Kashiwa, N.; Toda, Y. *J. Am. Chem. Soc.* **2002**, *124*, 1176. (c) Stehling, U. M.; Stein, K. M.; Fisher, D.; Waymouth, R. M. *Macromolecules* **1999**, *32*, 14. (d) Stehling, U. M.; Stein, K. M.; Kresti, M. R.; Waymouth, R. M. *Macromolecules* **1998**, *31*, 2019.

(5) (a) Chung, T. C. *CHEMTECH* **1991**, *21*, 496. (b) Chung, T. C. *Macromolecules* **1998**, *31*, 865.

(6) (a) Takeuchi, D.; Anada, K.; Osakada, K. *Macromolecules* **2002**, *35*, 9628. (b) Takeuchi, D.; Osakada, K. *Chem. Commun.* **2002**, 646. (c) Takeuchi, D.; Kim, S.; Osakada, K. *Angew. Chem., Int. Ed.* **2001**, *14*, 2685.

(7) For a preliminary communication on parts of this subject, see: Jensen, T. R.; Marks, T. J. *Macromolecules* **2003**, *36*, 1775.

opening to produce, via a new chain transfer mechanism, polymer **E** or **F** (depending on the catalyst).

E

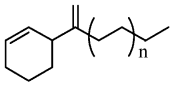

F

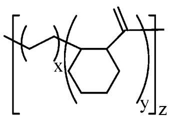

Experimental Section

Materials and Methods. All operations were performed with rigorous exclusion of oxygen and moisture in flame-dried Schlenk glassware on a dual-manifold Schlenk line or interfaced to a high-vacuum line (10^{-5} Torr) or in either a dinitrogen-filled Vacuum Atmospheres or MBraun glovebox with a high-capacity atmosphere recirculator (<1 ppm of O_2). Argon (Matheson, PP), ethylene (Matheson, CP), propylene (Matheson, PP), and dihydrogen (Linde) were purified by passage through a supported MnO oxygen-removal column and a Davison 4A molecular sieve column. Hydrocarbon solvents (toluene and pentane) were distilled under dinitrogen from Na/K alloy. All solvents were stored in vacuo over Na/K in Teflon valve-sealed bulbs. Deuterated solvents (all 99 atom % D) were purchased from Cambridge Isotope Laboratories, dried over Na/K alloy, vacuum-transferred into Teflon valve-sealed flasks, and freeze−pump−thaw degassed three times. The reagent 2-phenyl-2-propanol was purchased from Aldrich and dried under high vacuum for 3 h prior to use. The monomer 2-phenyl-1-methylenecyclopropane (**A**) was either purchased from Lancaster or synthesized by the literature procedure,[8] dried over CaH_2, freeze−pump−thaw degassed three times, and vacuum-transferred into a Teflon valve sealed storage flask. The synthesis of 7,7-dibromobicyclo[4.1.0]heptane has been previously reported.[9] The monomer 7-methylenebicyclo-[4.1.0]heptane (**B**) was prepared by a literature procedure,[10] dried over CaH_2, filtered, briefly (~10 min) dried, dehalogenated over Na/K, vacuum-transferred into a Teflon valve sealed storage flask, and freeze−pump−thaw degassed three times. The catalysts $Cp^*_2ZrMe^+MeB(C_6F_5)_3^-$, $Cp^*_2ZrMe^+B(C_6F_5)_4^-$, $(1,2\text{-}Me_2Cp)_2ZrMe^+B(C_6F_5)_4^-$, $Cp_2ZrMe^+B(C_6F_5)_4^-$, $[Cp^*_2LuH]_2$, $[Cp^*_2SmH]_2$, $Me_2Si(Me_4C_5)(^tBuN)ZrMe^+B(C_6F_5)_4^-$, and $Me_2Si(Me_4C_5)(^tBuN)TiMe^+B(C_6F_5)_4^-$ were prepared by following the procedures established in this laboratory.[11] The precatalysts $Cp^*_2ZrMe_2$, $Me_2Si(Me_4C_5)(^tBuN)ZrMe_2$, and $Me_2Si(Me_4C_5)(^tBuN)TiMe_2$ were prepared by following the published procedures.[12] The cocatalysts $B(C_6F_5)_3$ and $(C_6H_5)_3C^+B(C_6F_5)_4^-$ were prepared by following the published procedures.[13]

Physical and Analytical Measurements. NMR spectra were recorded on either a Varian Mercury 400 (FT, 400 MHz, ^1H; 100 MHz, ^{13}C; 376 MHz, ^{19}F) or an INOVA 500 (FT, 500 MHz, ^1H; 125 MHz, ^{13}C) spectrometer; CPMAS NMR spectra were recorded on a VXR-300 (FT, 300 MHz, ^1H; 75 MHz, ^{13}C) spectrometer. Chemical shifts for ^1H and ^{13}C spectra were referenced using internal solvent resonances and are reported relative to tetramethylsilane. CPMAS NMR spectra were referenced to adamantane. NMR experiments on air-sensitive samples were conducted in Teflon valve-sealed sample tubes (J. Young). DSC experiments were carried out on a TA Instruments DSC 2920 differential scanning calorimeter. TGA experiments were carried out on a TA Instruments SDT 2960 simultaneous DTA-TGA. GPC analyses of polymers were performed on a Waters Alliance GPCV 2000 (3 columns, Waters Styragel HT 6E, HT 4, HT 2; operation temperature, 140 °C; mobile phase, 1,2,4-trichlorobenzene; flow rate, 1 mL/min) and reported relative to six polyethylene standards (M_w, M_w/M_n: 119 600, 1.19; 32 100, 1.11; 13 600, 1.2; 2306, 1.14; 1214, 1.2; 800, 1.18) purchased from Polymer Laboratories. IR spectra were recorded using a Bio-Rad FTS-40 FT-IR spectrometer. Elemental analyses were preformed by Midwest Microlabs. Powder X-ray diffraction (XRD) data were collected every 0.05° for $5° < 2\theta < 25°$ and every 0.1° for $25° < 2\theta < 70°$ on a Rigaku diffractometer with Ni-filtered Cu Kα radiation.

Computational Details. All electronic structure calculations were carried out using Spartan 02 (Version 1.01, Wavefunction, Inc., Irvine, CA). In constructing the initial geometry model for a methyl-capped six-subunit oligomer of **D**, care was taken to provide a rational starting point and to explore different initial points. To construct the model, (1) the hydrogen atoms on the tertiary carbons of the bicyclo[4.1.0]heptane bridgehead were placed in a *syn*-disposed orientation, (2) the cyclohexyl rings were placed in chair conformations, and (3) the cyclopropyl rings of **D** were roughly orthogonal to the polymer backbone, and the *syn*-disposed hydrogen atoms across the cyclopropyl cyclohexyl bridgehead were all placed facing in the same direction relative to the polymer backbone.[14]

Two separate density functional theory B3LYP/6-31G* geometry optimizations were performed on the aforementioned six-subunit oligomers of **D** having different initial geometries. In the first case, a methyl-capped six-subunit oligomer of **D** was constructed. A constraint was added requiring that the distance between methyl caps be 15 Å, and the optimized geometry was then computed by molecular mechanics. The 15 Å constraint was then removed. This was the (linear) initial geometry of the DFT calculation (B3LYP/6-31G*). The methyl groups are 10.4 Å apart in the optimized geometry; this optimized geometry is shown in Figure 9. In the second case, the optimum geometry of one methyl-capped monomer unit of **B** was calculated (semiempirical PM3). One at a time, each unit of monomer **B** was added and the geometry was reoptimized (semiempirical PM3) after each addition until the six-subunit oligomer was complete. This result was then used as the initial geometry for the DFT calculation (B3LYP/6-31G*). The methyl groups are 6.7 Å apart in the optimized geometry.

Synthesis of Copolymer C. Representative Experiment. In the glovebox, a flame-dried three-neck Morton flask equipped with a large magnetic stir bar was charged with **A** (0.30 g, 2.31 mmol) and toluene (50 mL). The flask was attached to the high-vacuum line, and ethylene (1.0 atm) was introduced. The catalyst $[Cp^*_2LuH]_2$ (25 μmol of Lu) as a toluene solution was then injected into the reactor with rapid stirring. After 6 min, acidic methanol (20 mL) was injected to quench the reaction. Excess methanol was next used to precipitate the polymer. After filtration and washing, the polymer was dried under vacuum to constant weight to yield **C** (320 mg). A ^1H NMR spectrum of **C** is shown in Figure 2.

Synthesis of Poly(7-methylenebicyclo[4.1.0]heptane), Homopolymer D. In the glovebox, a flame-dried three-neck Morton flask equipped with a large magnetic stir bar was charged with **B** (0.67 g, 6.2 mmol) and toluene (50 mL). The flask was attached to the high-vacuum line and cooled to 0 °C. The catalyst $Cp^*_2ZrMe^+MeB(C_6F_5)_3^-$ (9 μmol) in toluene (2 mL) was injected into the reactor with rapid stirring. After

---

[8] (a) Arora, S.; Binger, P. *Synthesis* **1974**, 801. (b) Kitatani, K.; Hiyama, T.; Nozaki, H. *Bull. Chem. Soc. Jpn.* **1977**, *50*, 3288.

[9] Doering, W. V.; Hoffman, A. K. *J. Am. Chem. Soc.* **1954**, *76*, 6162.

[10] Salomon, R. G.; Sinha, A.; Salomon, M. F. *J. Am. Chem. Soc.* **1978**, *100*, 520.

[11] (a) Yang, X. M.; Stern, C. L.; Marks, T. J. *J. Am. Chem. Soc.* **1994**, *116*, 10015. (b) Jeske, G.; Schock, L. E.; Swepston, P. N.; Schumann, H.; Marks, T. J. *J. Am. Chem. Soc.* **1985**, *107*, 8091.

[12] (a) Manriquez, J. M.; McAlister, D. R.; Sanner, R. D.; Bercaw, J. E. *J. Am. Chem. Soc.* **1978**, *100*, 2716. (b) Kloppenburg, L.; Petersen, J. L. *Organometallics* **1997**, *16*, 3548. (c) Stevens, J. C.; Timmers, F. J.; Wilson, D. R.; Schmidt, G. F.; Nickias, P. N.; Rosen, R. K.; Knight, G. W.; Lai, S. Y. (to Dow Chemical) Eur. Pat. EP 416815 A2, 1991.

[13] (a) Massey, A. G.; Park, A. J. *J. Organomet. Chem.* **1964**, *2*, 245. (b) Chien, J. C. W.; Tsai, W.-M.; Rausch, M. D. *J. Am. Chem. Soc.* **1991**, *113*, 8570.

[14] Semiempirical calculations (PM3) produced indistinguishable results, regardless of the regiospecificity of the placement of the bridge protons relative to each other. They were placed all facing the same direction for simplicity in describing the model.

112 min, 20 mL of acidic methanol was injected to quench the reaction. Excess methanol was next used to precipitate the polymer. After filtration and washing (in no particular order) with benzene, water, chloroform, toluene, pentane, and methanol, the polymer was dried under vacuum to constant weight to yield 200 mg of **D**. Anal. Calcd for C_8H_{12}: C, 88.82; H, 11.18. Found: C, 88.93; H, 11.18. A CPMAS ^{13}C NMR spectrum of **D** is shown in Figure 4, an FTIR spectrum of this polymer is shown in Figure 5, and an XRD spectrum of the polymer is shown in Figure 7.

Cationic Polymerization of B. Similar to a procedure employed for the living cationic polymerization of isobutylene,[15] in the glovebox, a flame-dried three-neck Morton flask equipped with a large magnetic stir bar was charged with **B** (0.799 g, 7.4 mmol) and 2-phenyl-2-propanol (0.030 g, 220 μmol). The flask was attached to the high-vacuum line. Dichloromethane (6 mL) was next added by syringe. The reactor was placed in a cold bath, and the temperature of the reactor was equilibrated to −20 °C. The catalyst BCl_3 (2.2 g, 1.88 mmol) was injected into the reactor with rapid stirring. After 30 min, precooled methanol (20 mL) was injected to quench the reaction. Excess methanol was then used to precipitate the polymer, and the polymer was triturated for 24 h. After filtration and washing with methanol, the polymer was dried under vacuum to constant weight to yield 90 mg of polymer. The ^{13}C NMR spectrum of this polymer is shown in Figure 8.

Synthesis of Capped Polymer E. Representative Experiment. In the glovebox, a flame-dried three-neck Morton flask equipped with a large magnetic stir bar was charged with **B** (0.30 g, 185 mmol) and toluene (50 mL). The reactor was attached to the high-vacuum line, and ethylene (1.0 atm) was introduced. After the temperature had stabilized, $Cp^*_2ZrMe^+B(C_6F_5)_4^-$ (25 μmol) in toluene (2 mL) was injected with rapid stirring. After 0.25 min, acidic methanol (20 mL) was injected to quench the reaction. Next, methanol (400 mL) was added and the polymer was allowed to precipitate overnight. The polymer was then filtered, washed with methanol, and dried under vacuum to constant weight, yielding **E** (702 mg).

Synthesis of 7,7-Dimethylbicyclo[4.1.0]heptane (G). This compound has been previously prepared.[16] It was synthesized by a method similar to that for an analogous compound starting from 7,7-dibromobicyclo[4.1.0]heptane.[17] To a suspension of dry copper(I) cyanide (8.56 g, 95.8 mmol) in diethyl ether (150 mL) was added MeLi (109 mL of a 1.6 M solution in diethyl ether, 174 mmol) at −78 °C. The mixture was gradually warmed to 0 °C over 45 min. The mixture was then cooled to −30 °C, and a solution of 7,7-dibromobicyclo[4.1.0]heptane (2.2 g, 8.7 mmol) and HMPA (3.8 mL, 8.7 mmol) in diethyl ether (150 mL) was added dropwise. Stirring was continued for an additional 45 min (the temperature was allowed to rise to −15 °C), after which time MeI (30 mL) was added. The mixture was stirred for another 5 min and then poured into a mixture of saturated aqueous NH_4Cl (180 mL) and concentrated NH_4OH (20 mL). The two-phase mixture was separated, and the aqueous layer was extracted with two portions of CH_2Cl_2 (100 mL). The combined organic layers were washed with brine and dried over $MgSO_4$. Distillation afforded 0.55 g (50% yield) of pure product; bp 70 °C at 70 Torr. ^1H NMR ($CDCl_3$): δ 0.53 (m, 1 H), 0.54 (m, 1 H), 0.95 (s, 3H), 0.97 (s, 3H), 1.18 (m, 4H), 1.35 (m, 2H), 1.82 (m, 2H).

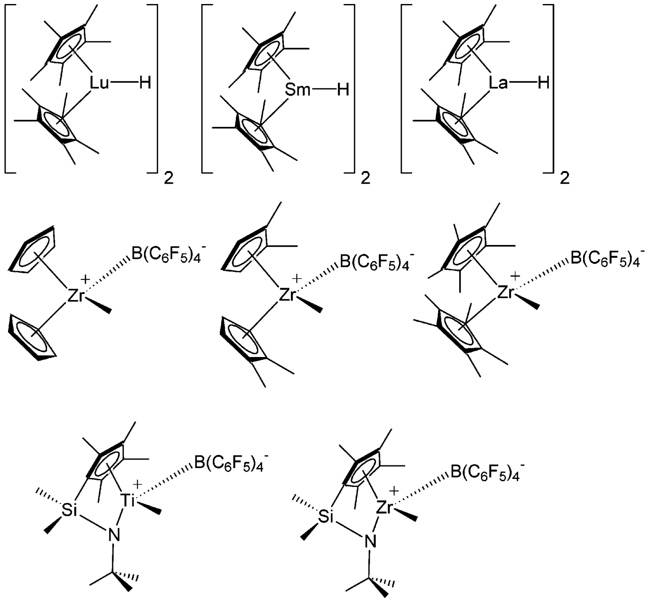

Figure 1. Catalysts examined for ROZP activity.

Results and Discussion

The goal of this study was to examine the viability of ROZP with a variety of catalysts (shown in Figure 1) for mono- and disubstituted methylenecyclopropanes and, if successful, to examine mechanistic aspects of the polymerization. The first section presents results on the homo- and copolymerization of monomer **A**, a monosubstituted methylenecyclopropane, which readily undergoes copolymerization with ethylene to form polymer **C** in the presence of a number of electrophilic homogeneous single-site polymerization catalysts. Next, the selective ring-unopened homopolymerization of monomer **B**, a disubstituted bicyclic methylenecyclopropane, to form polymer **D** is discussed. The final section presents the various pathways available in ethylene copolymerizations with monomer **B**. A full discussion of the pathways available, including formation of the ring-opened **B**-capped polymer **E** and random ring-opened **B** + ethylene copolymers **F**, as well as the kinetics of these processes, reveals an instructive, thought-provoking general picture of ROZP reaction pathways.

2-Phenyl-1-methylenecyclopropane (A) Polymerization and Copolymerization Characteristics. To date, all efforts to produce a homopolymer of monomer **A** with group IV or lanthanide catalysts have been unsuccessful. All of the catalysts shown in Figure 1 were screened under dilute and concentrated conditions of monomer **A** and at ambient temperatures and 0 °C. In contrast to the negative homopolymerization results, a variety of lanthanocene catalysts and one zirconocene catalyst effect the efficient copolymerization of **A** + ethylene in a ring-opened fashion to form atactic copolymer **C**. Table 1 summarizes the results for the various catalysts; all polymerizations were carried out with a pseudo-zero-order excess of **A**. A priori, following 1,2-insertion of **A,** the ring opening via β-alkyl elimination at the cyclopropyl ring can proceed via either of two possible pathways to yield polymer **C** (eq 7). Pathway i (Scheme 1) should be favored by electronic coordinative factors such as η^6-phenyl ring coordination to the electrophilic metal center. The result is similar to the 2,1-insertion regiochemistry observed in styrene homopolymerizations and in styrene copolymerizations with ethylene.[18] Steric factors placing the primary rather than secondary cyclopropyl carbon on the metal

---

[15] Mishra, M. K.; Chen, C. C.; Kennedy, J. P. *Polym. Bull.* **1989**, *22*, 455.

[16] Corey, E. J.; Posner, G. H. *J. Am. Chem. Soc.* **1967**, *89*, 3911.

[17] Jenniskens, L. H. D.; Wijnberg, J. B. P. A.; Groot, A. D. *J. Org. Chem.* **1991**, *56*, 6585.

Table 1. Data for Copolymerizations of 2-Phenyl-1-methylenecyclopropane (A) and Ethylene To Form Polymer C[a]

entry	catalyst	amt of **A** (mmol)	reacn time (min)	polymer yield (mg)	activity[b]	M_n (M_w/M_n)	T_m (°C)	ratio in polymer of ethylene/monomer **A**[d]
1	$(Me_5Cp)_2ZrMe_2$[e]	2.3	5	90	43	7500 (2.3)	122	130
2	$[(Me_5Cp)_2LuH]_2$	2.3	6	320	128	22 430 (2.1)	133	340
3	$[(Me_5Cp)_2YH]_2$	2.3	6	350	140	24 970 (2.1)	134	>1000
4	$[(Me_5Cp)_2SmH]_2$	2.3	6	100	40	10 880 (2.1)	131	540

[a] Polymerizations carried out with ethylene (1 atm, 0.19 mol/L)[20] at 20 °C in toluene (50 mL) with catalyst (25 μmol in metal); polymerizations carried out with pseudo-zero-order excess concentration of monomer **A**. [b] In units of 10^3 g of polymer/((mol of catalyst) atm h). [c] By GPC in 1,2,4-trichlorobenzene at 140 °C versus polyethylene standards. [d] Determined by ^{1}H NMR. [e] Catalyst (25 μmol) and $(C_6H_5)_3C^+B(C_6F_5)_4^-$ (28 μmol) used.

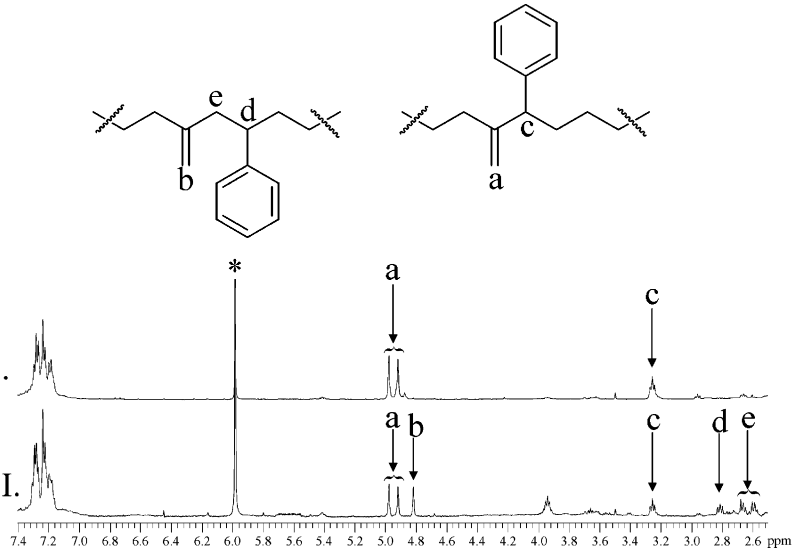

Figure 2. 500 MHz ^{1}H NMR spectra in $C_2D_2Cl_4$ at 125 °C of copolymer **C**: (I) **A** + ethylene polymerization mediated by $Cp^*_2ZrMe^+B(C_6F_5)_4^-$; (II) **A** + ethylene polymerization mediated by $[Cp^*_2SmH]_2$. The asterisk denotes a solvent resonance.

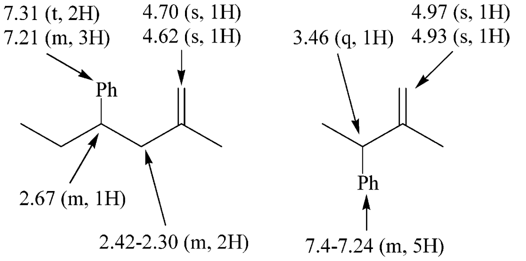

Figure 3. ^{1}H NMR assignments (δ) of small-molecule models of polymer **C**.[18]

Scheme 1. The Two Possible Ring-Opening Pathways for Monomer A

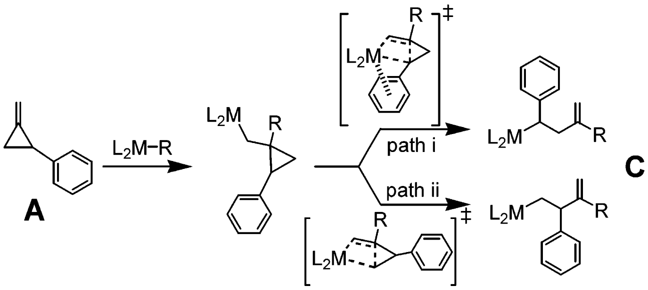

Scheme 2. Proposed Catalytic Cycle for Organolanthanide-Mediated Intermolecular Hydroamination of 2-Phenyl-1-methylenecyclopropane (A)

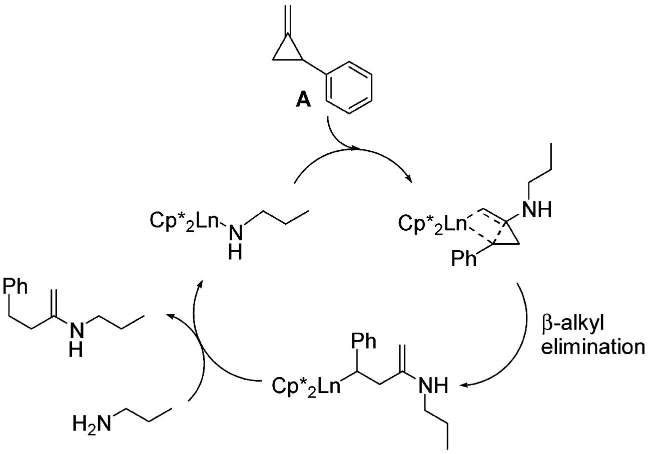

center should favor pathway ii (Scheme 1). The ^{1}H NMR spectra of two **C**-derived polymer samples produced with different catalysts are shown in Figure 2 (from Table 1, entries 1 and 4). They clearly reveal that ring opening can proceed by either pathway, with different catalysts exhibiting different selectivities for either pathway i or pathway ii (the NMR assignments were made on the basis of parameters for known model organic compounds and are shown in Figure 3).[19] Note that the most sterically congested catalyst, $Cp^*_2ZrMe^+B(C_6F_5)_4^-$, follows path ii in Scheme 1 almost exclusively (the more

---

(18) (a) Oliva, L.; Caporaso, L.; Pellecchia, C.; Zambelli, A. *Macromolecules* **1995**, *28*, 4665. (b) Pellecchia, C.; Pappalardo, D.; D'Arco, M.; Zambelli, A. *Macromolecules* **1996**, *29*, 1158.

(19) (a) Rubin, M.; Gevorgyan, V. *Org. Lett.* **2001**, *3*, 2705. (b) Schwink, L.; Knochel, P. *Chem. Eur. J.* **1998**, *4*, 950.

Scheme 3. Two Potential Isomerization Ring-Opening Pathways for Monomer A

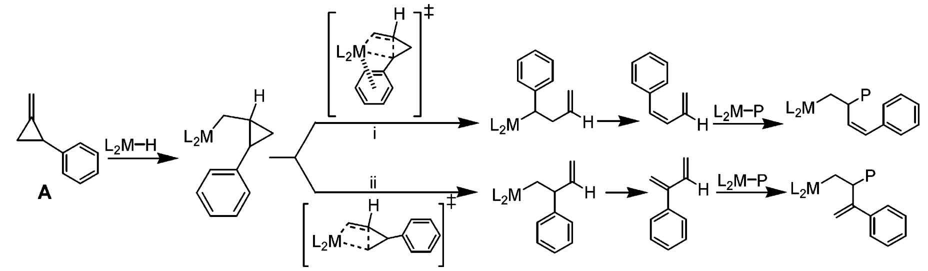

sterically favorable pathway). In contrast, the less sterically crowded organolanthanide catalysts mediate both pathways, with the larger ionic radius metal, Sm, promoting pathway i with ~30% selectivity and the smaller ionic radius metal, Lu, mediating pathway i with ~10% selectivity. This result stands in contrast to intermolecular organolanthanide-catalyzed hydroamination studies with **A**, where ring opening occurs exclusively such that the phenyl carbon atom is located adjacent to the lanthanide center after β-alkyl elimination (Scheme 2).[20]In the case of [Cp*$_2$SmH]$_2$, the intermolecular hydroamination is greater than 90% selective for ring opening similar to pathway i, whereas in ethylene copolymerizations with **A**, [Cp*$_2$SmH]$_2$ is only ~30% selective for pathway i, Scheme 1.

With regard to the mechanism, it is conceivable that **A** could undergo reaction with a catalyst metal–hydride functionality (derived either from the starting catalyst or following β-hydride elimination of the growing polymer chain) and then undergo isomerization to yield a ring-opened isomer, which was subsequently enchained during the polymerization (Scheme 3). This possibility can be discounted for two reasons. First, judging from the low incorporation level of **A** (~1%), a combination of the low concentration of **A** versus ethylene (1:4.3)[21] and/or the difference in the rate of insertion of the two olefins into a metal–alkyl bond results in an observed rate of ethylene insertion over monomer **A** insertion that is at least 100× faster. It is also likely that the observed rate difference is paralleled in olefin insertion into a metal–hydride bond. Therefore, it is reasonable that very little **A** ever undergoes reaction with a metal hydride. This mechanistic contention is further supported by the fact that GC/MS analysis of the supernatant after a copolymerization reaction reveals only **A** and no other isomers of **A**. Second, the ^{1}H NMR spectrum of polymer **C** is inconsistent with the enchainment of either of the hypothetical structures formed in Scheme 3.

It is also found that the **A** + ethylene copolymerization reactions are relatively sluggish compared to ethylene homopolymerizations carried out under identical conditions with the same catalysts (~1–3 orders of magnitude slower).[11] Product molecular weights are also substantially lower than in analogous ethylene homopolymerizations;[11] however, polydispersities remain ~2, in accord with a single-site, nonliving polymerization process. Generally, the incorporation level of comonomer **A** is modest (~ 1% for all catalysts by ^{1}H NMR). This level is less than the previously reported incorporation levels of methylenecyclopropane in ethylene copolymerizations mediated by these same catalysts under similar reaction conditions.[3] Presumably the additional bulk of the phenyl group renders insertion less favorable relative to methylenecyclopropane.

Table 2. Data for Polymerizations of 7-Methylenebicyclo[4.1.0]heptane (B)

entry	catalyst	temp (°C)	amt of **B** (mmol)	reacn time (min)	polymer yield (mg)	activity[a]	T_m (°C)
1[b]	(Me$_5$Cp)$_2$ZrMe$_2$[d]	0	6.2	112	200	11900	>310
2[c]	BCl$_3$	−20	7.4	30	90	820	n.d.

[a] In units of g of polymer/((mol of catalyst) h). [b] Polymerization carried out in toluene (50 mL) with catalyst (9 μmol) and B(C$_6$F$_5$)$_3$ (12 μmol). [c] Polymerization carried out in CH$_2$Cl$_2$ (6 mL), BCl$_3$ (1.88 mmol), and 2-phenyl-2-propanol (220 μmol).

Ring-Unopened Polymerization of 7-Methylenebicyclo[4.1.0]heptane (B). Polymerization of **B** mediated by the sterically encumbered metallocenium catalyst Cp*$_2$ZrMe$^+$MeB(C$_6$F$_5$)$_3^-$ at 0 °C results in *ring-unopened* product **D** (Table 2), as will be discussed below. Interestingly, this material is insoluble in all solvents investigated, even at high temperatures. Because of the insolubility, structural characterization of **D** was carried out by solid-state CPMAS ^{13}C NMR, DSC, elemental analysis, FTIR, TGA, and XRD. Ring opening of the product resulting from enchainment of **B** via β-alkyl elimination should produce an *exo*-methylene functionality (eq 9);[3] however, the solid-state CPMAS ^{13}C NMR spectrum of **D** (Figure 4) reveals no resonances assignable to unsaturated carbon centers (no signals downfield of δ 50 ppm). A dipolar dephasing pulse experiment[22] indicates that there is a quaternary ^{13}C resonance at δ 22 ppm, consistent with a ring-closed structure, whereas the quaternary ^{13}C after *ring opening* would be olefinic (eq 9). In addition, the FTIR spectrum of **D** exhibits no absorptions corresponding to ν(C=C) modes; the 1500–2500 cm^{-1} region is featureless. Indeed, the FTIR and CPMAS NMR spectral parameters are very similar to those reported for the saturated hydrocarbon 7,7-

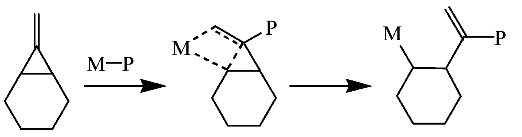

(9)

---

[20] Ryu, J.-S.; Li, Y.; Marks, T. J. *J. Am. Chem. Soc.* **2003**, *125*, 12584.

[21] For ethylene solubility data in toluene see: Wang, B. P. Ph.D. Dissertation, University of Massachusetts, 1989.

[22] Schmidt-Rohr, K. S.; Spiess, H. W. *Multidimensional Solid-State NMR and Polymers*; Academic Press: London, San Diego, 1994; p 71.

[23] IR of **G**: (a) Andrews, E. D.; Harvey, W. E. *J. Chem. Soc.* **1964**, 4636. NMR of **G**: (b) Schlosser, M.; Chau, L. V.; Spahić, B. *Helv. Chim. Acta* **1975**, *58*, 2575. (c) Francesco, F.; Gottlieb, H. E.; Hagaman, E. W.; Taticchi, A.; Wenkert, E.; Wovkulich, P. M. *Gazz. Chim. Ital.* **1975**, *105*, 1215.

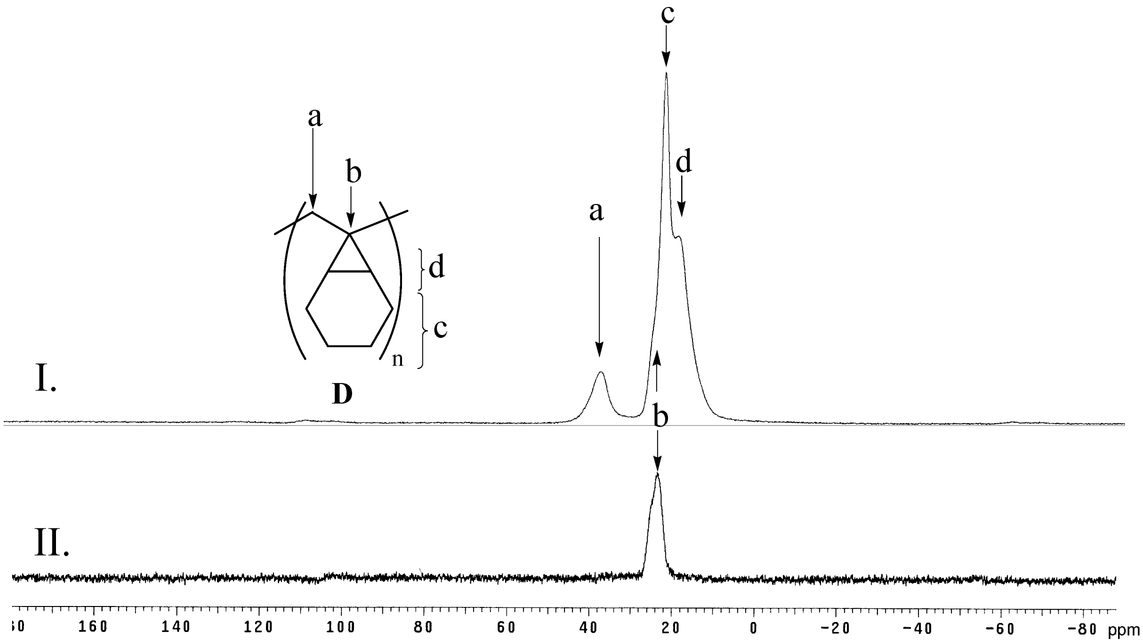

Figure 4. (I) CPMAS ^{13}C NMR spectrum (6.5 kHz, 20 000 transients) of polymer **D** (there are spinning sidebands at δ ~109 and ~−64 ppm). (II) Dipolar dephasing[22] CPMAS ^{13}C NMR spectrum (6.5 kHz, 8500 transients) of polymer **D** (there are spinning sidebands at δ ~102 and ~−55 ppm).

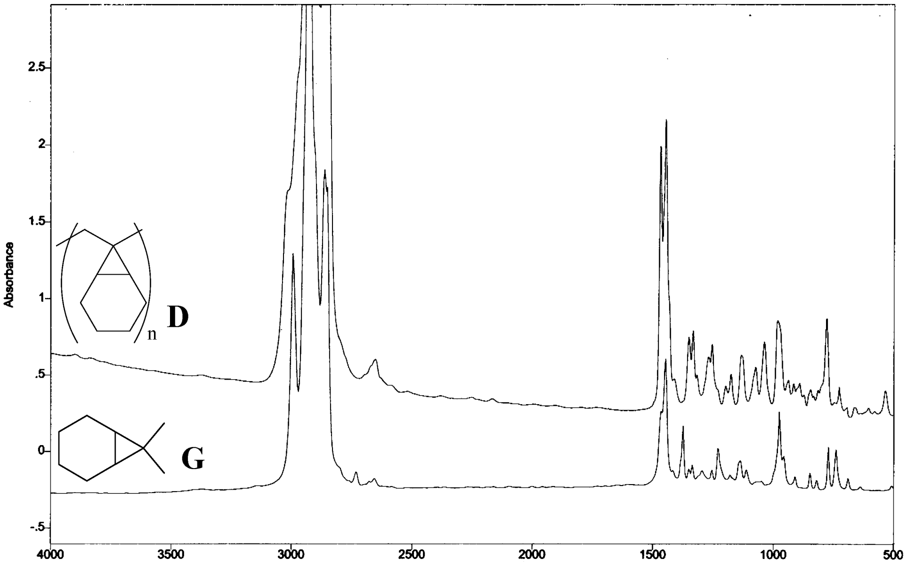

Figure 5. Overlayed FTIR spectra of polymer **D** and compound **G**.

dimethylbicyclo[4.1.0]heptane (**G**);[23] the FTIR spectral

G

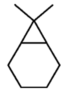

similarity between polymer **D** and small molecule **G** is shown in Figure 5. Spectral broadening typically associated with solid-state NMR renders the 1,2-insertion vs 2,1-insertion regioselectivity and tacticity assignments uncertain. For steric reasons, a 1,2-insertion pathway seems most probable, since 2,1-insertion places a bulky cyclohexyl carbon directly on the metal center.[24]

DSC and TGA data show that **D** undergoes decomposition prior to melting, with decomposition beginning at ~310 °C; other hydrocarbon polymers with $T_m > T_{decomp}$ are known, including some polycycloolefins.[25] TGA data for **D** reveal ~5% weight loss by 363 °C (10 °C/min ramp rate under N$_2$); DSC data exhibit no features until a large decomposition exotherm at ~310 °C (10 °C/min ramp rate). The low T_{decomp} of this hydrocarbon polymer (cf. polyethylene with 5% weight loss at 459 °C; see Figure 6)[26] is further evidence that the majority of **B** cyclopropyl rings remain intact during the polymerization. Two other polymers with enchained

---

(24) Attempts to produce a trimer or oligomer using dihydrogen for chain transfer have been unsuccessful.

(25) Kaminsky, W. *J. Chem. Soc., Dalton Trans.* **1998**, *9*, 1413.

(26) Polyethylene produced under identical conditions as **A** (same catalyst, solvent, and temperature, but under 1.0 atm of ethylene instead of **A**).

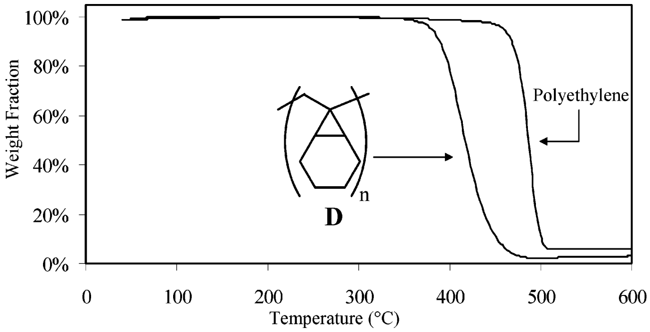

Figure 6. TGA profiles of polymer **D** and polyethylene[26] (ramp rate 10 °C/min).

cyclopropyl rings, poly(3-ethyl-3-methylcyclopropene)[27] (**H**) and ring-unopened Ni-catalyzed poly(2-phenyl-1-methylenecyclopropane)[6] (**I**), exhibit similar thermal properties (~5% weight loss at 330 °C reported for **H**). Unlike polymer **H**,[28] the FTIR spectra and TGA data for **D** remain unchanged over 20 months under ambient conditions. X-ray powder diffraction data (Ni-filtered Cu Kα radiation) for **D** exhibit two sharp reflections at 2θ = 9.33 and 17.32°, with full-width at half-maximum values of 2.26 and 2.76°, respectively, indicating partial crystallinity, lattice repeat spacings of ~9.55 and ~5.12 Å, respectively, and an average particle size/coherence length of ~35 Å (Figure 7).[29] It is not presently known whether the process which produces **D** is living; ring opening of **A** during the polymerization could provide a pathway for termination through β-hydride elimination/chain transfer. The insolubility of **D** precludes GPC analysis to determine molecular weight and polydispersity, and spectral signatures for end-group features in the CPMAS NMR or FTIR spectra of **D** are below the detection limits.

H

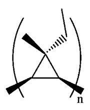

I

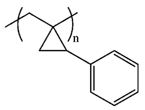

In principle, the polymerization pathway which forms polymer **D** could be either cationic (owing to the structural similarity between monomer **B** and isobutylene) or coordinative/insertive. Differentiation between these mechanisms can be nontrivial.[30] Initial observations support the coordinative/insertive mechanism in the formation of polymer **D**. In the cationic polymerization of isobutylene, both $Cp_2ZrMe^+MeB(C_6F_5)_3^-$ and $Cp^*{}_2ZrMe^+MeB(C_6F_5)_3^-$ are reported to be effective initiators at temperatures below −30 °C.[31] However, for monomer **B,** $Cp_2ZrMe^+MeB(C_6F_5)_3^-$ is completely ineffective for initiating polymerization, and the formation of **D** is efficient at much higher temperatures (~0 °C). To further eliminate any possibility that this polymerization follows a cationic pathway, the cationic polymerization of **B** was investigated with a system known to initiate living isobutylene cationic polymerization (BCl_3 + 2-phenyl-2-propanol).[15] The results are shown in Table 2, entry 2. The first notable difference versus the metallocenium-mediated process

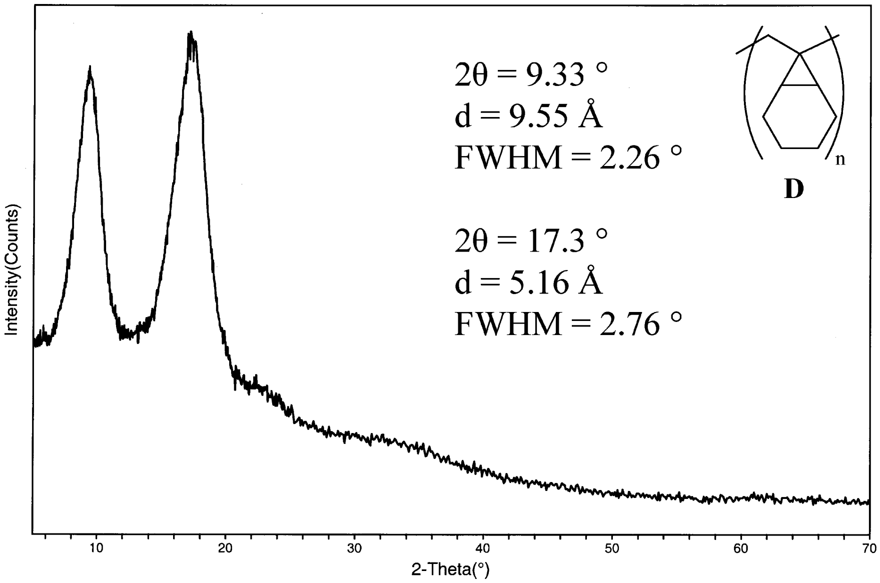

Figure 7. $\theta - 2\theta$ X-ray powder diffraction pattern of polymer **D** on an amorphous silica substrate.

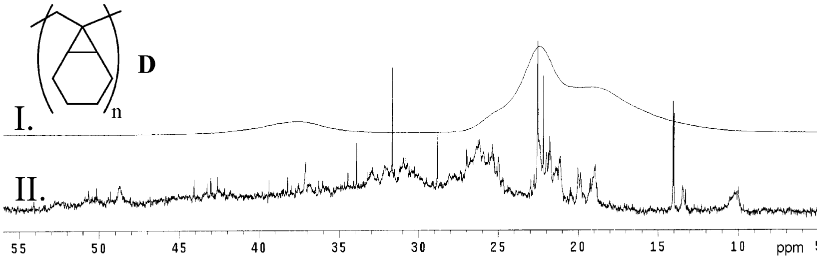

Figure 8. Two NMR spectra: (I) solid-state 75 MHz ^{13}C CPMAS NMR spectrum of **D** (6.5 kHz, 20 000 transients); (II) solution 125 MHz ^{13}C NMR (in $CDCl_3$) of the polymer formed from the cationic polymerization of monomer **B** initiated by BCl_3 + 2-phenyl-2-propanol.

is that the **B**-derived polymer obtained from the cationic system is very soluble (in toluene at room temperature). Comparison of the solution ^{13}C NMR spectrum of the cationically derived polymer with the solid-state ^{13}C CPMAS NMR of **D** (Figure 8) clearly shows the two polymers to be very different microstructurally. In the cationic polymerization, it is quite clear from both the ^{13}C NMR and GC/MS analysis of the low-molecular-weight species in solution that substantial isomerization (ring opening) of **B** has taken place. This is not surprising, since the cationic rearrangement of the norcarane structure has ample literature precedent.[32] In one particular example involving the acid-promoted cationic rearrangements of bicyclo[4.1.0]heptane and 7-methylbicyclo[4.1.0]heptane, it was reported that product formation followed both pathway A (~23%, eq 10) and pathway B (~77%, eq 10) for bicyclo[4.1.0]heptane (R = H, eq 10).[33] Similarly for 7-methylbicyclo[4.1.0]heptane (R = CH_3, eq 10), ~53% follows pathway A and ~47% pathway B (eq 10).[33] Therefore, it seems almost certain that the carbocations present in a cationic polymerization of monomer **B** would undergo ring opening. Indeed, as noted above, numerous isomers of **B** are detectable in the supernatant GC/MS during the cationic polymerization of **B** (all **B** is consumed; none is detectable by GC/MS). In contrast, no isomers of **B** are observed in the GC/MS analysis of the supernatant in the metallocene-catalyzed reaction mixture that forms polymer **D**. This evidence persuasively *rules out* the formation of **D** via a classical cationic polymerization pathway.

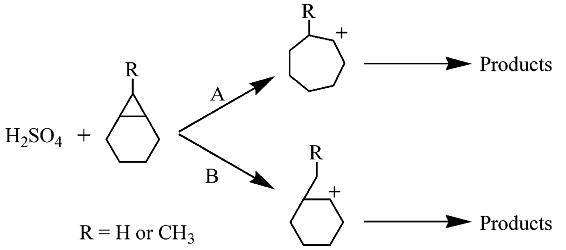

(10)

A computational study was also undertaken to better understand the macromolecular structure of polymer **D**. The optimized geometry (density functional theory at the B3LYP/6-31G* level; see Experimental Section for details) of a six-subunit oligomer capped with a methyl group to make the chain ends identical is shown in Figure 9. The molecule was initially constructed as a linear polymer; upon energy minimization, it collapsed to the more compact configuration shown in Figure 9. Note that the methyl chain ends are only 10.4 Å apart. In contrast, the corresponding chain ends in two similar calculations performed on model oligomers of polyethylene and syndiotactic polystyrene (the optimized geometries are almost perfectly linear) are found to be 15.38 and 15.05 Å apart, respectively. We speculate that this collapsed optimized geometry of polymer **D** (Figure 9) is connected with this polymer's insolubility and high melting point. Apparently, these large bicyclo[4.1.0]heptane units with only single methylene spacers between them are too crowded to allow sufficient free movement and rotation for dissolution. We propose this also explains the ~10 ppm downfield shift of the methylene spacer in the CPMAS ^{13}C NMR spectrum (Figure 4, the peak marked "a" at ~36 ppm). One possible explanation that is consistent with the insolubility, high melting point, partial crystallinity, and optimized geometry of this polymer would be that polymer **D** has a roughly helical structure.[34] The structure shown in Figure 9 is consistent with a helical conformation.

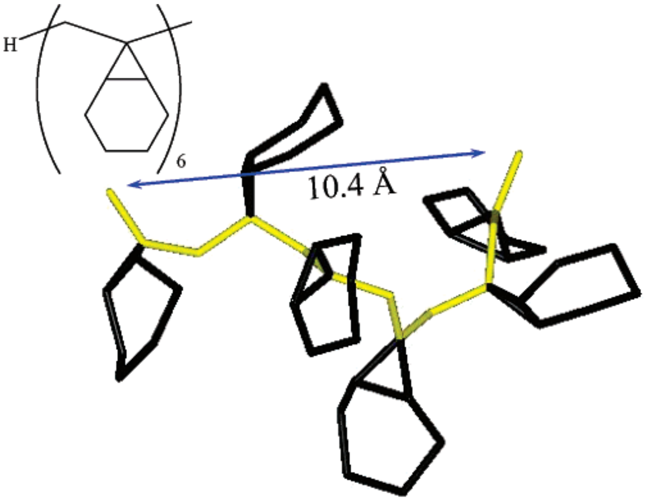

Figure 9. Geometry-optimized B3LYP/6-31G*-derived structure of polymer **D** (six units of monomer **B** plus one methyl group at the chain end). The hydrogen atoms have been eliminated for clarity. The computed distance between the oligomer chain ends is shown. The polymer backbone is yellow, and the bicyclo[4.1.0]heptane units are black.

In addition to contributing to the insolubility of polymer **D,** the steric bulk of bicyclic monomer **B** is likely responsible for the unique ring-unopened microstructure of **D**. Methylenecyclopropane has >40 kcal/mol of strain energy, and monomer **B** is likely to possess similar or greater strain.[35] However, it is enchained in a *ring-unopened* manner. Of all the catalysts in Figure 1 examined for polymerization activity with respect to **B** (at 0 and 20 °C), only the most sterically encumbered catalyst, $Cp^*_2ZrMe^+MeB(C_6F_5)_3^-$, is significantly active, and even then only at ~0 °C. This suggests that with more coordinatively "open" catalysts and at higher temperatures, ring opening occurs rapidly following 1,2-insertion of **B** (eq 9). After ring opening, the next step should be either chain propagation or chain termination. The propagation step would then be enchainment of an 1,1-disubstituted olefin (**B**) into a metal−cyclohexyl ring bond (eq 11). Judging from the reactivity of single-site

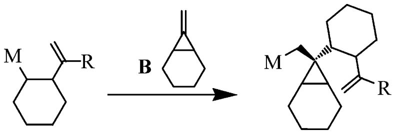

(11)

---

[27] Rush, S.; Reinmuth, A.; Risse, W.; O'Brien, J.; Ferro, D. R.; Tritto, I. *J. Am. Chem. Soc.* **1996**, *118*, 12230.

[28] Over 7 months ~70% of the cyclopropyl rings in **F** are reported to undergo opening under ambient conditions.[27]

[29] Average particle size/coherence length as expressed by the Scherrer equation in: Alexander, L. E. *X-ray Diffraction Methods in Polymer Science*; Wiley: New York, 1969; pp 335−337.

[30] Baird, M. C. *Chem. Rev.* **2000**, *100*, 1471 and references therein.

[31] Carr, A. G.; Dawson, D. M.; Bochmann, M. *Macromolecules* **1998**, *31*, 2035.

[32] Newcomb, M.; Shen, R.; Lu, Y.; Coon, M. J.; Hollenberg, P. F.; Kopp, D. A.; Lippard, S. J. *J. Am. Chem. Soc.* **2002**, *124*, 6879.

[33] LaLonde, R. T.; Tobias, M. A. *J. Am. Chem. Soc.* **1964**, *86*, 4068.

Table 3. Data for Copolymerizations of 7-Methylenebicyclo[4.1.0]heptane (B) and Ethylene[a]

entry	catalyst	amt of **B** (mmol)	reacn time (min)	polymer yield (mg)	activity[b]	M_n (M_w/M_n)[c]	T_m (°C)	ratio in polymer of ethylene/monomer	polymer formed
1	$(Me_5Cp)_2ZrMe_2$	2.8	0.25	702	6739	2190 (1.8)	123	84	**E**
2	$(Me_5Cp)_2ZrMe_2$	5.6	0.5	873	4190	1800 (1.5)	117	46	**E**
3	$(Me_5Cp)_2ZrMe_2$	11.1	0.5	503	2414	1420 (1.3)	108	23	**E**
4	$CGCZrMe_2$	2.8	1	227	545	2 520 (2.2)	127	50	**F**
5	$CGCZrMe_2$	5.6	3	153	122	1780 (1.4)	123	23	**F**
6	$CGCZrMe_2$	11.1	10	161	39	1450 (1.2)	70	13	**F**
7	$CGCZrMe_2$	2.8	2	1183	1420	16 360 (2.2)	118	470	**F**
8	$CGCZrMe_2$	5.6	3	663	530	8250 (1.8)	none	160	**F**
9	$CGCZrMe_2$	11.1	7	244	84	6760 (1.8)	none	66	**F**
10	$[(Me_5Cp)_2LuH]_2$[e]	2.8	0.5	455	2184	36130 (1.6)	136	>1000	**F**
11	$[(Me_5Cp)_2LuH]_2$[e]	5.6	1	246	590	23330 (1.9)	136	>1000	**F**
12	$[(Me_5Cp)_2LuH]_2$[e]	11.1	1	148	355	21510 (1.9)	136	>1000	**F**

[a] Polymerizations carried out in toluene (50 mL) at 20 °C with catalyst (25 μmol), $(C_6H_5)_3C^+B(C_6F_5)_4^-$ (28 mmol), and ethylene (1.0 atm, 0.19 mol/L);[20] polymerizations carried out with pseudo-zero-order excess concentration of monomer **B**. [b] In units of 10^3 g of polymer/((mol of catalyst) atm h). [c] By GPC in 1,2,4-trichlorobenzene at 140 °C versus polyethylene standards. [d] Determined by ^{1}H NMR. [e] No cocatalyst and 25 μmol of Lu used.

Scheme 4. Perspective Drawings of the Ring-Opening Step (β-Alkyl Elimination) for Methylenecyclopropane (Top) and Bicyclic Monomer B (Bottom)[a]

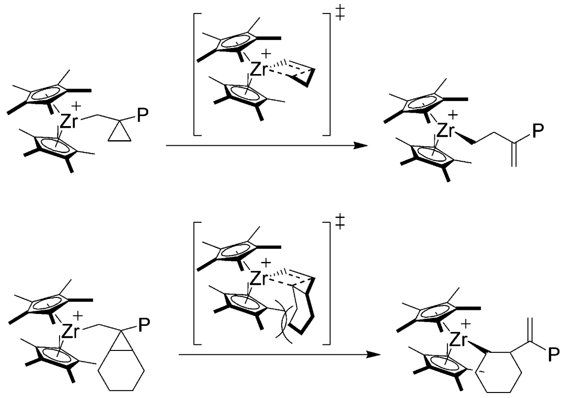

[a] The counteranion is deleted for clarity.

Scheme 5. Proposed Catalytic Cycle for the Copolymerization of B + Ethylene

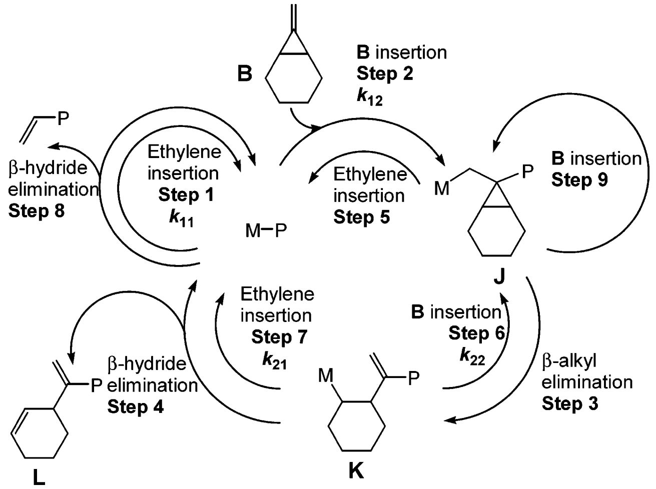

catalysts with other 1,1-disubstituted olefins,[36] this step should be extremely slow, and this is probably the reason the majority of catalysts examined fail to effect the homopolymerization of **B**. In contrast to eq 11, Cp*$_2$ZrMe$^+$MeB(C$_6$F$_5$)$_3^-$ at low temperatures disfavors ring opening. Scheme 4 shows that repulsive nonbonded interactions between the cyclohexyl ring of **B** and the catalyst Cp* ligand occur in formation of the four-membered transition state required for β-alkyl elimination.[37] In summary, at low temperatures, the bulky catalyst Cp*$_2$ZrMe$^+$MeB(C$_6$F$_5$)$_3^-$ cannot effect ring opening for steric reasons and instead catalyzes the coordinative/insertive formation of ring-unopened macromolecule **D**.

Ethylene Copolymerizations with 7-Methylenebicyclo[4.1.0]heptane (B). Copolymerizations of monomer **B** with ethylene mediated by a variety of d^0/f^n catalysts afford either polymer **E** or **F** (vide supra), depending on the catalyst. Polymerization data are summarized in Table 3. Representative ^{1}H and ^{13}C NMR spectra of polymer **E** are shown in Figure 10, and the ^{1}H NMR spectrum of polymer **F** is shown in Figure 11. All copolymerizations were carried out with a pseudo-zero-order excess of monomer **B**. A proposed polymerization mechanism for the formation of copolymers **E** and **F** is shown in Scheme 5.

The formation of polymer **E** mediated by Cp*$_2$ZrMe$^+$B(C$_6$F$_5$)$_4^-$ is the simplest process to understand. The catalyst effects ethylene polymerization in a standard Ziegler pathway (step 1, Scheme 5), until monomer **B** is eventually enchained (step 2, Scheme 5). At that point, structure **J** (Scheme 5) can either undergo olefin insertion (step 5 or 9, Scheme 5) or β-alkyl elimination (step 3, Scheme 5). At room temperature, intramolecular ring opening (step 3, Scheme 5) appears to predominate over intermolecular olefin enchainment (step 5 or 9, Scheme 5; this is observed for all catalysts examined). After step 3, structure **K** (Scheme 5) can either undergo olefin insertion (step 6 or 7, Scheme 5), or β-hydride elimination (step 4, Scheme 5). For the catalyst Cp*$_2$ZrMe$^+$B(C$_6$F$_5$)$_4^-$ at room temperature, only step 4 (Scheme 5) is observed. These processes (steps 1–4, Scheme 5) readily achieve formation of polymer **E**. There are in principle two possible pathways for the β-hydride elimination/chain transfer (step 4, Scheme 5), but because the bridgehead C–H units of **B** are *syn*-disposed, only

---

(34) See the following and references therein: Nakano, T.; Okamoto, Y. *Chem. Rev.* **2001**, *101*, 4013.

(35) Schleyer, P. v. R.; Williams, J. E.; Blanchard, K. R. *J. Am. Chem. Soc.* **1970**, *92*, 2377.

(36) Shaffer, T. D.; Canich, J. A. M.; Squire, K. R. *Macromolecules* **1998**, *31*, 5145.

(37) (a) Watson, P. L.; Parshall, G. W. *Acc. Chem. Res.* **1985**, *18*, 51. (b) Bunel, E.; Burger, B. J.; Bercaw, J. E. *J. Am. Chem. Soc.* **1988**, *110*, 976. (c) Eshuis, J. W.; Tan, Y. Y.; Teuben, J. H. *J. Mol. Catal.* **1990**, *62*, 277. (d) Resconi, L.; Piemontesi, F.; Franciscono, G.; Abis, L.; Fiorani, T. *J. Am. Chem. Soc.* **1992**, *114*, 1025.

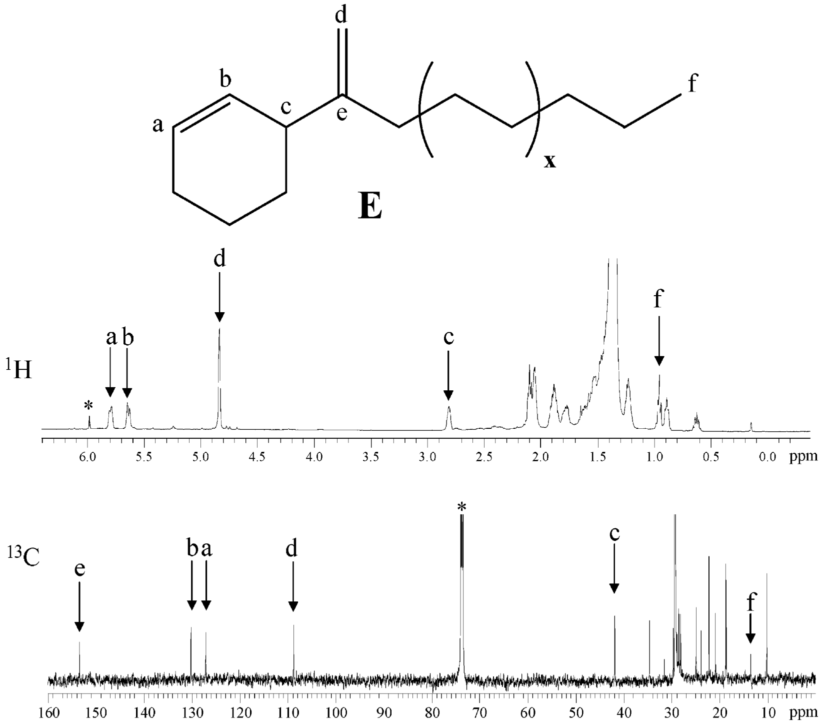

Figure 10. 500 MHz ^{1}H and 125 MHz ^{13}C NMR spectra of copolymer **E** in $D_2Cl_4C_2$ at 125 °C. The asterisk denotes the solvent resonance.

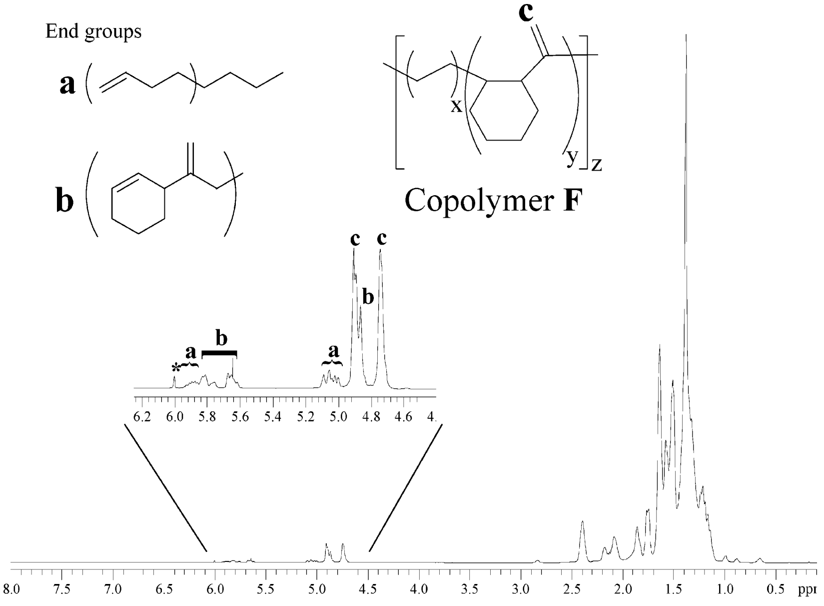

Figure 11. 500 MHz ^{1}H NMR spectrum of the copolymer **F** (Table 3, entry 4) in $D_2Cl_4C_2$ at 125 °C.

product **E** is observed (eq 12). Essentially, the hydride that would produce the conjugated double bond (the hydride on the tertiary carbon of the cyclohexyl ring) is *trans*-disposed with respect to the metal (eq 12) and therefore unavailable for β-hydride elimination/chain transfer.

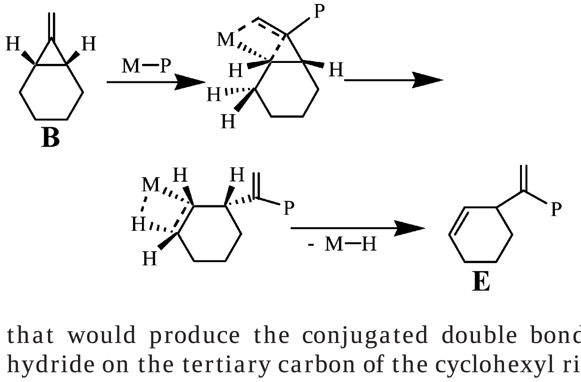

(12)

The formation of polymer **E** is quite rapid (Table 3, entries 1−3), with activity only slightly depressed relative to the homopolymerization of ethylene. Although it is clear that monomer **B** does depress the activity (compare entries 1−3; as the concentration of monomer **B** is increased the activity decreases), the product molecular weight is also substantially depressed by addition of monomer **B**. The thermal properties of polymers **E** are generally as expected. The T_m values are low (relative to HDPE at ~136 °C);[38] however, the relative contribution of low molecular weight (M_n <

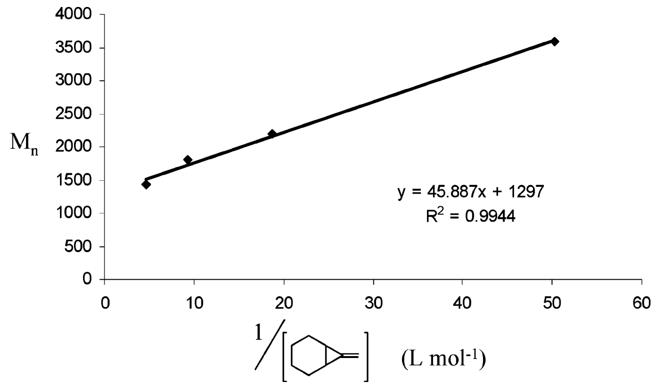

Figure 12. Relationship of polymer **E** number-average molecular weight (GPC versus polyethylene) to the concentration of chain-transfer agent **B** for fixed catalyst, $Cp^*_2ZrMe^+B(C_6F_5)_4^-$, and ethylene concentrations.[41]

3000) versus **B** incorporation level cannot be unambiguously differentiated. The end group produced by step 8 (Scheme 5) is below the detection limit (Figure 10). Essentially, monomer **B**, in concert with this catalyst, is acting as a chain transfer agent. Assuming constant catalyst, olefin, and chain transfer concentrations and that the majority of **B** insertions lead to chain transfer, $\bar{P}_n$ at the operational steady state should obey eq 13,

$$\bar{P}_n = \frac{k_p[\text{olefin}]}{k_B[\mathbf{B}] + k_{ct'}[\mathrm{Y}]^x} \qquad (13)$$

where $\bar{P}_n$ is the number average degree of polymerization, k_p is the rate of propagation, k_B is the rate of chain transfer by monomer **B**, and $k_{ct'}[\mathrm{Y}]^x$ takes into account other possible competing chain transfer processes.[39] In the present study, polymerizations were carried out with constant catalyst, ethylene, and **B** concentration (**B** is maintained in pseudo-zero-order excess). From eq 13, there should be a linear relationship between M_n and $[\mathbf{B}]^{-1}$ in cases where participation of steps 6 and 7 is insignificant.[39] In accord with the aforementioned observations that the rate of steps 6 and 7 in macromolecule growth is negligible when $Cp^*_2ZrMe^+B(C_6F_5)_4^-$ is employed as the catalyst,[40] Figure 12 shows that the expected linear relationship of $[\mathbf{B}]^{-1}$ to M_n is observed in the formation of polymer **E**. As expected, as $[\mathbf{B}]^{-1}$ approaches 0, $M_n \rightarrow \sim 110$.[41] From the data in Figure 12 and using eq 13, $k_p/k_B \approx 25$. This number is significantly lower than the values reported for organosilane chain transfer agents ($k_p/k_B \approx 130$ for $PhSiH_3$ with ethylene and $[Cp^*_2SmH]_2$, and $k_p/k_B \approx 35$ for $PhSiH_3$ with propylene and $Me_2Si(Me_4C_5)(^tBuN)TiMe^+B(C_6F_5)_4^-$).[39a,42] Apparently, with $Cp^*_2ZrMe^+B(C_6F_5)_4^-$ as the catalyst, monomer **B** acts as an effective chain transfer agent.

A kinetic analysis provides information about the rate of ethylene insertion, k_{11}, versus the rate of **B** insertion, k_{12}. The rate equations for ethylene insertion and **B** insertion are shown in eqs 14 and 15, respectively. In

$$-\frac{d[\text{ethylene}]}{dt} = k[\mathrm{M-P}][\text{ethylene}] \qquad (14)$$

$$-\frac{d[\mathbf{B}]}{dt} = k_{12}[\mathrm{M-P}][\mathrm{B}] \qquad (15)$$

the formation of polymer **E**, steps 5–9 (Scheme 5) are not observed; as a result, the observed rate difference in ethylene and monomer **B** incorporation can be determined simply from the difference in their incorporation quantities in polymer **E**. Combining eqs 14 and 15 and solving for k_{12}/k_{11} yields eq 16, where the

$$\frac{k_{12}}{k_{11}} = \frac{\frac{d[\mathrm{B}]}{dt}[\text{ethylene}]}{\frac{d[\text{ethylene}]}{dt}[\mathbf{B}]} \qquad (16)$$

observed rate ratio $[(d[\mathbf{B}]/dt)/(d[\text{ethylene}]/dt)]$ is equal to the ratio of monomer **B** to ethylene incorporated in polymer **D** (Table 3). Therefore, according to eq 16,[43] $k_{12}/k_{11} = 0.04(\pm 0.005)$. This result demonstrates that the rate of incorporation of the 1,1-disubstituted olefin, monomer **B**, is ~25× slower than the rate of ethylene incorporation. While, on a thermodynamic Hammond postulate basis,[44] one might expect monomer **B** to undergo more rapid insertion (specifically, the insertion of methylenecyclopropane into a metal–alkyl bond (similar to step 2, Scheme 5) is estimated to be ~8 kcal /mol more exothermic than ethylene insertion (similar to step 1, Scheme 5)),[45] clearly, steric factors dominate, and ethylene inserts more rapidly than bulky monomer **B**. A priori, one might predict that a bulky 1,1-disubstituted monomer such as **B** would be significantly less reactive than ethylene, and it is likely that the extra thermodynamic driving force accounts for some of the similarity in rate.

Although the result that $k_{11} > k_{12}$ in **B** + ethylene copolymerization is expected, it is still reassuring that data derived from GPC and ^1H NMR are in agreement on this issue. In the production of polymer **E**, chain transfer invariably follows insertion of monomer **B**. As a result, k_{12} (from Scheme 5) must be equal to k_B (from eq 11). Therefore, in this picture, $k_{12}/k_{11} = [k_p/k_B]^{-1}$. This internal check proves reassuringly to be true, and k_{12}/k_{11} (^1H NMR derived) $\approx [k_p/k_B]^{-1}$ (GPC derived) ≈ 0.04. There is also agreement between polymer molecular weights determined by GPC and by ^1H NMR. It is evident by ^1H NMR that one monomer **B** is incorporated

---

(38) Boenig, H. V. *Structure and Properties of Polymers*; Georg Thieme: Stuttgart, Germany, and Wiley: New York, 1973; p 19.

(39) (a) Koo, K.; Marks, T. J. *J. Am. Chem. Soc.* **1999**, *121*, 8791. (b) Tait, P. J. T.; Watkins, N. D. In *Comprehensive Polymer Science*; Allen, G., Bevington, J. C., Eds.; Pergamon Press: Oxford, U.K., 1989; Vol. 4, p 549.

(40) The ^1H NMR spectrum of polymer **E** shows >95% of all end groups to consist of ring-opened monomer **B** (Figure 10).

(41) The plot does not pass directly through ~110 g/mol (the formula mass of the monomer). This offset we believe is due to two factors. First, especially at lower molecular weights, the GPC calibration based on linear polyethylene probably is not strictly valid, since the ring-opened **B** fragment represents a significant fraction of the polymer microstructure. Second, the GPC column set is less accurate at lower molecular weights and results in slightly overestimated molecular weights and underestimated polydispersities. Notice that for polymers with $M_n < 5000$, generally the value of $M_w/M_n < 2$ (Table 3). We believe this is a consequence of poor separation of low-molecular-weight polymers and not a true narrowing of polymer polydispersity.

(42) (a) Koo, K.; Fu, P.-F.; Marks, T. J. *Macromolecules* **1999**, *32*, 981. (b) Koo, K.; Marks, T. J. *J. Am. Chem. Soc.* **1998**, *120*, 4019.

(43) The concentration of **B** is given in Table 3, and for the concentration of ethylene, see ref 20.

(44) (a) Carroll, F. A. *Perspectives on Structure and Mechanism in Organic Chemistry*; Brooks/Cole: New York, 1998; pp 254–256. (b) Hammond, G. S. *J. Am. Chem. Soc.* **1955**, *77*, 334.

(45) For a full discussion of the thermodynamics, see ref 3a.

per chain in polymer **E**. The average ratio of ethylene to monomer **B** enchained in polymer **E** can be determined by integration of the ^{1}H NMR spectrum (results are shown in Table 3). This allows a straightforward determination of molecular weight by ^{1}H NMR and yields molecular weight values of 2460, 1400, and 750 (for Table 3, entries 1−3, respectively). These determinations are in excellent agreement with the GPC-derived M_n values of 2190, 1800, and 1420 (Table 3, entries 1−3, respectively).

Unfortunately, no comparisons can be drawn between the present k_{12}/k_{11} value for **B** + ethylene → **E** and our previous results for methylenecyclopropane + ethylene copolymerizations[3] or to **A** + ethylene copolymerization to form copolymer **C**. This is because unless steps 5−9 (Scheme 5) are known to be of negligible importance, the observed analysis is rather complex, and k_{12}/k_{11} cannot be straightforwardly derived. While we cannot determine k_{12}/k_{11} for other ethylene copolymerization systems, it is not unreasonable to suspect that the value we have determined approaches a lower limit for k_{12}/k_{11}. This is because, in the present system, monomer **B** is the most sterically bulky monomer investigated to date, and $Cp^*{}_2ZrMe^+B(C_6F_5)_4^-$ is the most sterically encumbered catalyst employed for these polymerizations (see Figure 1). Therefore, it is reasonable to suppose that k_{12}/k_{11} determined for polymer **E** formation is the lowest of all the systems encountered to date.

Efficient formation of copolymer **F** is effected by three catalysts, $[Cp^*{}_2LuH]_2$, $Me_2Si(Me_4C_5)(^tBuN)ZrMe^+B(C_6F_5)_4^-$, and $Me_2Si(Me_4C_5)(^tBuN)TiMe^+B(C_6F_5)_4^-$ (Table 3, entries 4−12). Scheme 5 explains the formation of polymer **F**. The principal difference between formation of copolymers **E** and **F** is that, with these more sterically "open" catalysts, steps 6 and 7 (Scheme 5) are now potentially accessible. Similar to the situation for copolymer **E**, increasing the concentration of monomer **B** depresses activity for copolymer **F** formation. The trend in molecular weight is the same for all three catalysts; as monomer **B** concentration increases, copolymer M_n falls, although $M_w/M_n \approx 2$, consistent with single-site behavior. The thermal properties of copolymer **F** are generally as expected. Thus, the T_m values of the products in entries 10−12 of Table 3 are similar to that of normal HDPE (~136 °C),[46] largely because these products have $M_n > 10\,000$ and contain >99% ethylene. The products of entries 4−9 of Table 3 have lower T_m values (relative to HDPE); however, the relative contributions of low molecular weight ($M_n < 17\,000$) versus **B** incorporation level cannot be unambiguously differentiated.

The proposed mechanism of formation of polymer **F** is evident from Scheme 5. By ^{1}H NMR spectroscopy (Figure 11) it is clear that monomer **B** has been enchained in an atactic ring-opened fashion in the polymer backbone (structure **M**). There is also some quantity of ring-opened end capping of monomer **B** in polymer **F** (structure **L**). The formation of polymer **F** is proposed to begin via normal ethylene enchainment (step 1, Scheme 5). Eventually, monomer **B** is enchained in step 2 (Scheme 5). As observed before for polymer **E** formation (vide supra), intramolecular *β*-alkyl elimination (step 3, Scheme 5) dominates over olefin enchainment at room temperature (steps 5 and 9, Scheme 5) for all catalysts. Once at structure **K** (Scheme 5), the cationic alkyl can undergo *β*-hydride elimination (step 4) to terminate chain growth and form a metal hydride or undergo further olefin insertion (step 6 or 7). The presence of structure **M** in the polymer backbone argues that either step 6 (k_{21}) or step 7 (k_{22}) must occur. The fact that $k_{21} > 0$ and/or $k_{22} > 0$ prevents the simple analysis of k_{12}/k_{11} that was carried out for polymer **E** formation above. As explained earlier, this is because the observed **B**:ethylene ratio in polymer **F** reflects the interplay of greater than two rates. However, there is still kinetic information to be gleaned from this polymer formation process. By ^{1}H NMR, the **M**:**L** ratio can be determined. For catalyst $Me_2Si(Me_4C_5)(^tBuN)ZrMe^+B(C_6F_5)_4^-$, **M**:**L** = 7.4, 7.7, and 6.9 (Table 3, entries 4−6, respectively). Clearly, therefore, for this catalyst, the **M**:**L** ratio is zero-order in monomer **B** concentration. This result implies that, for $Me_2Si(Me_4C_5)(^tBuN)ZrMe^+B(C_6F_5)_4^-$, step 6 in Scheme 5 must be negligible; i.e., $k_{22} = 0$. In contrast, for the catalyst $Me_2Si(Me_4C_5)(^tBuN)TiMe^+B(C_6F_5)_4^-$, **M**:**L** = 1.6, 3.3, and 8.0 (Table 3, entries 7−9, respectively). Therefore, for the catalyst $Me_2Si(Me_4C_5)(^tBuN)TiMe^+B(C_6F_5)_4^-$, the **M**:**L** ratio is approximately first-order in monomer **B** concentration, indicating that, for this catalyst, the rate of step 6 must be appreciable ($k_{22} > 0$), which is a surprising result. Note that in the variable-concentration studies, $Me_2Si(Me_4C_5)(^tBuN)ZrMe^+B(C_6F_5)_4^-$ incorporates more **B** relative to ethylene than does $Me_2Si(Me_4C_5)(^tBuN)TiMe^+B(C_6F_5)_4^-$, for a given **B** concentration. The most obvious explanation for this ordering is the larger ionic radius of Zr^{4+} vs Ti^{4+}, and thus the rate of bulky monomer **B** enchainment is greater at the less sterically congested catalyst. Although this explanation is plausible, it leaves unanswered the question of why the more "open" catalyst, $Me_2Si(Me_4C_5)(^tBuN)ZrMe^+B(C_6F_5)_4^-$, which displays a greater preference for monomer **B** enchainment, exhibits $k_{22} = 0$, while less "open" $Me_2Si(Me_4C_5)(^tBuN)TiMe^+B(C_6F_5)_4^-$ exhibits $k_{22} > 0$. One rationalization for this intriguing observation involves counteranion mobility. Anion effects are known to impact many aspects of homogeneous single-site olefin polymerization in nonpolar media and include significant consequences for catalyst activity, lifetime, stability, chain-transfer characteristics, and stereoregulation.[1a,47] For monomer **B**, it is possible that, following insertion and ring opening to produce intermediate structure **K** (Scheme 5), the fused cyclohexyl ring at the Ti center weakens the cation−anion ion pairing.[48] This would lower the barrier to either ethylene or monomer **B** insertion (step 6 or 7, Scheme 5). It must be argued then that this anion reorganization is unnecessary for the larger Zr catalyst, or possibly that ethylene insertion is rapid prior to this ion pair weakening (the Zr catalyst is more "open"), and

L

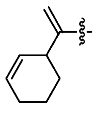

M

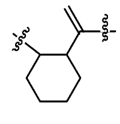

---

[46] Boenig, H. V. *Structure and Properties of Polymers*; Georg Thieme: Stuttgart, Germany, and Wiley: New York, 1973; p 19.

[47] (a) Chen, E. Y.-X.; Marks, T. J. *Chem. Rev.* **2000**, *100*, 1391. (b) Chen, M.-C.; Marks, T. J. *J. Am. Chem. Soc.* **2001**, *123*, 11803.

[48] Stahl, N. G.; Zuccaccia, C.; Jensen, T. R.; Marks, T. J. *J. Am. Chem. Soc.* **2003**, *125*, 5256.

thus a rapid ethylene insertion (step 7) circumvents anion reorganization, leading to $k_{22} = 0$ for $Me_2Si(Me_4C_5)(^tBuN)ZrMe^+B(C_6F_5)_4^-$. There is precedent for ion pair weakening by sterically encumbered, metal-bound alkyl groups in metallocenium catalysis.[49]

The catalyst $[Cp*_2LuH]_2$ produces copolymer **F** with the highest molecular weight, and $[Cp*_2LuH]_2$ exhibits the lowest incorporation level of monomer **B** (for a given **B** concentration). That $[Cp*_2LuH]_2$ has the lowest **B** incorporation selectivity is not unexpected, since it has been demonstrated that *ansa*-bridged lanthanocenes are efficient catalysts for 1-hexene + ethylene copolymerizations but that their nonbridged analogues are significantly less efficient.[11b,39] As a consequence, the product polymers have high molecular weights and low incorporation levels of monomer **B**, with the high molecular weight rendering microstructure analysis necessarily imprecise. The ^1H NMR spectral signatures of **F** are observed but are near the detection limits, while end-group information is below the detection limits. Nevertheless, there should be no doubt that monomer **B** is incorporated with these catalysts; addition of monomer **B** depresses the product molecular weight by an order of magnitude relative to the corresponding ethylene homopolymerization,[11b] and increasing the monomer **B** concentration depresses the polymer M_n (Table 3, entries 10−12).

In principle, all of the present catalysts should be competent to effect the skeletal isomerization of **B**, and it might be assumed that if **B** were to react with a metal hydride and undergo isomerization, then the product isomer (**N**) could be incorporated into the polymer chain (eq 17). This possibility can be ruled out by two lines of argument. First, judging from the low incorporation level of **B** (<7.7%; Table 3), a combination of the low concentration of **A** versus ethylene (1:(0.89−3.6); Table 3)[21] and/or the difference in the rate of insertion of the two olefins into a metal-alkyl bond ($k_{11} = 25k_{12}$ for polymer **E** formation) results in a higher observed rate of ethylene insertion over monomer **B**. This argues that the observed rate of insertion of **B** into a metal−hydride bond should be significantly less than ethylene insertion. This assertion is supported by the fact that GC/MS analysis of the supernatant after a polymerization reaction shows no evidence of the **B** isomers. As a result, there should not be significant concentrations of isomer **N** available in solution to be enchained. Furthermore, if a process similar to eq 17 were operative, then the expected ^1H NMR integration ratios (Figure 10) would become (a + b) > d. This is clearly not the case, and the ratios are as expected for formulation **E** or **F** via the process in Scheme 5, with (a + b):d being 1:1.

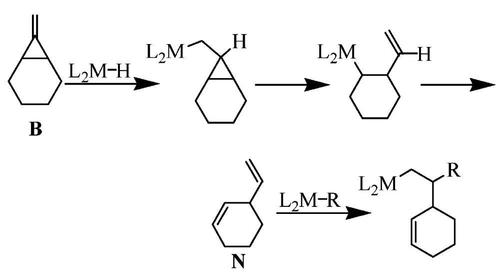

(17)

The results of the present ethylene and monomer **B** copolymerizations are in good accord with our previous findings with methylenecyclopropane.[3] Activities and incorporation rates are similar. For both systems, the group 4 polymerization catalysts exhibit higher activities and comonomer incorporation rates than the organolanthanide catalysts. Unlike methylenecyclopropane, which undergoes copolymerization in the presence of all of the organolanthanide catalysts, the bicyclic monomer **B** only undergoes copolymerization by the lanthanocene with the smallest ionic radius metal, Lu^{3+}. Presumably, the larger ionic radius metals incorporate monomer **B** to such an extent that the polymerization is greatly retarded (steps 4, 6, and 7 of Scheme 5 are slow), and termination processes dominate. Similarly, the present work also reveals that monomer **B** only undergoes polymerization in the presence of the most sterically congested zirconocene, $Cp*_2ZrMe^+B(C_6F_5)_4^-$, while the more "open" $Cp_2ZrMe^+B(C_6F_5)_4^-$ and $(1,2\text{-}Me_2C_5H_3)_2ZrMe^+B(C_6F_5)_4^-$ are ineffective.

Conclusions

The scope of ring-opening Ziegler polymerization has now been expanded to include mono- and 2,3-disubstituted methylenecyclopropanes. Overall, polymerization activities and comonomer incorporation levels are diminished slightly relative to those of unsubstituted methylenecyclopropane. It is interesting that there are two possible pathways for an unsymmetrical monosubstituted methylenecyclopropane to undergo β-alkyl elimination via Scheme 2, and in the case of $Cp*_2ZrMe^+B(C_6F_5)_4^-$, monomer **A** can very selectively follow a single pathway (>95%, pathway ii). In contrast, as noted above, late-transition-metal (Ni) catalysts are very selective for homopolymerization of **A** in a ring-unopened mode and another Ni catalyst has been shown to incorporate **A** with a mixture of ring-opened and ring-unopened structures.[6] Interestingly, the Pd and Ni catalysts do not appear to be selective with regard to the regiochemistry of cyclopropyl ring opening, and a number of methylene resonances are observed in their ^1H NMR spectra.[6a,c] Methylenecyclopropanes have greater than 40 kcal/mol of ring strain,[35] which is a major factor driving the ring-opening process in ROZP homo- and copolymerizations.[3] Thus, it is not surprising that the majority of enchained monomers were found to undergo ring opening in all previous studies with methylenecyclopropanes or methylenecyclobutanes.[3,50] In the present case, it is surprising that monomer **B** affords a homopolymer, **D**, with *negligible ring opening*; proper selection of catalyst and temperature are key to effecting this transformation. Similarly, the choice of catalyst in ethylene copolymerizations with monomer **B** allows selection of the capped polyethylene product **E** or a random copolymer of ring-opened monomer **B** + ethylene (polymer **F**). Note that the formation of copolymer **E** represents (to our knowledge) a new type of

---

(49) (a) Beswick, C. L.; Marks, T. J. *J. Am. Chem. Soc.* **2000**, *122*, 10358. (b) Zuccaccia, C.; Macchioni, A.; Stahl, N. G.; Marks, T. J. *J. Am. Chem. Soc.*, in press.

(50) The ring-unopened polymerization of methylenecyclobutane mediated by a heterogeneous catalyst has been proposed (Pinazzi, C. P.; Brossas, J. *Makromol. Chem.* **1969**, *122*, 105), and very recently Ni-catalyzed ring-unopened polymerization of 2-phenyl-1-methylenecyclopropane has been reported.[6a,b]

chain transfer mechanism, initiated by a monomer that undergoes insertion and subsequently undergoes isomerization to a structure, which then triggers chain termination (presumably by blocking additional olefin insertion). Monomer **B** also presents an interesting example of a chain transfer agent that is actually incorporated into the polymer prior to terminating chain growth, while simultaneously creating a new reactive end group. Of particular interest also is that polymer **E** formation allows determination of the difference in ethylene vs monomer **B** enchainment rate constants (ethylene undergoes insertion ∼25× faster than monomer **B**). Monomers **A** and **B** demonstrate that new pathways previously unobserved in ROZP are accessible and include ring-unopened polymerizations as well as polyolefin capping. More generally, **A** and **B** indicate that ROZP is a very general pathway that functions for both unsubstituted and substituted methylenecyclopropanes.

Acknowledgment. We thank the NSF (Grant No. CHE-0078998) and the DOE (Grant No. 86ER13511) for support of this research. We thank Dr. H. Ahn for CPMAS NMR assistance and S. J. Barry and Dr. J. T. Rijssenbeek for XRD assistance.

OM030407N